Collective excitations in ^{33}S

Abhijit Bisoi,[1] M. Saha Sarkar,[1,*] S. Sarkar,[2] S. Ray,[1] D. Pramanik,[2] R. Kshetri,[1,†] Somnath Nag,[3] K. Selvakumar,[3] P. Singh,[3] A. Goswami,[1] S. Saha,[4] J. Sethi,[4] T. Trivedi,[4] B. S. Naidu,[4] R. Donthi,[4] V. Nanal,[4] and R. Palit[4]

[1]*Saha Institute of Nuclear Physics, Bidhannagar, Kolkata 700064, India*

[2]*Indian Institute of Engineering Science and Technology, Shibpur, Howrah 711103, India*

[3]*Indian Institute of Technology, Kharagpur 721302, India*

[4]*Tata Institute of Fundamental Research, Mumbai 400005, India*

(Received 15 May 2014; revised manuscript received 15 July 2014; published 29 August 2014)

High spin states of ^{33}S populated through ^{27}Al(^{12}C,αpn)^{33}S reaction at $E(^{12}\mathrm{C}) = 40$ MeV have been studied using the Indian National Gamma Array (INGA) facility. The level scheme was extended and modified utilizing data from the γ-γ coincidence, directional correlation, and linear polarization measurements. Three levels of the negative parity yrast sequence were found to be connected by strong $E2$ transitions. The lifetimes of these states determined by the Doppler shift attenuation method have been utilized to study the evolution of collectivity with spin. Large basis shell model calculations have been performed to understand the microscopic origin of these levels.

DOI: 10.1103/PhysRevC.90.024328 PACS number(s): 21.10.Re, 21.10.Tg, 21.60.Cs, 27.30.+t

I. INTRODUCTION

Recently, several sophisticated experiments [1–5] and state-of-the-art theoretical calculations [2,3,6] have been performed to understand the spectroscopic properties of nuclei in the upper-*sd* shell. Nuclei in this region usually exhibit characteristics of spherical single particle excitations [1,7] at low spins. While at higher spins, states of pure single particle nature have been found to coexist with those with strong collectivity. This evolution of excitation modes with increasing spins as well as coexistence at higher spins are also well explained by shell model calculations.

$^{33}S_{17}$, a stable nucleus in the upper-*sd* shell was found to be quite interesting. Measured quadrupole moments of the first 2^+ excited state in $^{32}S_{16}$ indicates a prolate deformation. On the other hand, ^{33}S itself has a ground state quadrupole moment corresponding to an oblate shape [8]. Therefore, this change in shape with inclusion of one neutron indicates their "softness" [9]. Superdeformed (SD) configurations with cluster structures in ^{32}S and other neighboring nuclei like ^{33}S, ^{31}S, have been a topic of intense theoretical studies [10–12]. However, apart from indications that these SD states in ^{32}S may exist from the measurements in the $^{16}\mathrm{O} + {}^{16}\mathrm{O}$ breakup channel ($E_{\mathrm{threshold}}$) $\simeq$ 16.5 MeV [13]), by the molecular resonances, from inelastic α scattering at extremely forward angles for ($^{28}\mathrm{Si} + \alpha$) cluster structure ($E_{\mathrm{threshold}} \simeq 6.9$ MeV) [14], no clear evidence for these SD bands in ^{32}S was reported from gamma spectroscopic studies. However, similar SD states have been identified in ^{35}Cl [3], ^{36}Ar [4], ^{40}Ca [5], and ^{28}Si [15] indicating clusterization with fragments of unequal masses. Thus, one may expect to find deformed cluster bands in the excitation spectra of ^{33}S generated by coupling a neutron to SD states in ^{32}S ($E_{\mathrm{threshold}} \simeq 8.6$ MeV) or coupling an α to ^{29}Si ($E_{\mathrm{threshold}} = \simeq 7.1$ MeV).

Coexistence of collective and single particle excitations have generated new interest in this mass region [3]. In a recent work in ^{34}Cl [2], collective excitations were observed at higher excitation energy. In ^{35}Cl [3] also, a negative parity band was observed which evolves from single particle excitation [$B(E2) \simeq 5$ W.u.] at low spins to collective and superdeformation [$B(E2) \simeq 20-33$ W.u.] at high spins. Therefore, the aim of the present work is to extend the level scheme to higher spins and study the evolution of collectivity with increasing spin in ^{33}S. This study may be useful for planning new experiments in the search for superdeformation in this nucleus.

Earlier the excitation spectra of ^{33}S have been extensively studied [1] through proton, light ions, and alpha-beam-induced reactions. However, only one study includes data from a heavy-ion-induced reaction [16]. In the present work, a fusion evaporation reaction with heavy ion beams was used to populate ^{33}S. Data from the γ-γ coincidence, and intensity measurements have been analyzed to extend and modify the existing level scheme. Multipolarity, mixing ratios, and the nature of several γ transitions have been measured or reconfirmed by directional correlation ratio (DCO) and polarization measurements. The lifetimes of a few levels have been estimated from lineshape analysis. Large basis shell model (LBSM) calculations have been performed for different truncations to understand the microscopic origin of these levels.

II. EXPERIMENTAL DETAILS AND DATA ANALYSIS

High spin states of ^{33}S have been populated through the ^{27}Al(^{12}C, αpn)^{33}S reaction. The ^{12}C beam of 40-MeV energy was delivered by the 14-UD Pelletron accelerator at Tata Institute of Fundamental Research (TIFR), Mumbai. The target consisted of 0.50 mg/cm^2 ^{27}Al with 10 mg/cm^2 gold backing to stop the recoils. γ -γ coincidence measurement was done using the multidetector array of 15 Compton suppressed Clover detectors (INGA setup) [17]. The detectors were placed

*maitrayee.sahasarkar@saha.ac.in

†Present address: Sidho-Kanho-Birsha University, Purulia 723101, India.

at 157° (3), 140° (2), 115° (2), 90° (4), 65° (2), and 40° (2) with respect to the beam axis. Other necessary details of the setup have been discussed in Ref. [2].

The energy calibration and high energy efficiency calibration of the Clover detectors have been done using ^{133}Ba, ^{152}Eu, and ^{66}Ga sources. The radioactive ^{66}Ga ($T_{1/2} = 9.41$ h) source was prepared through ^{56}Fe(^{13}C,p2n)^{66}Ga reaction at 50 MeV using the same setup [2].

III. RESULTS AND DISCUSSION

A. Level scheme

The experimental data have been sorted into angle-independent and -dependent (90° vs 90°) symmetric γ-γ matrices. The level scheme of ^{33}S was extended up to ≈8 MeV on the basis of coincidence relationship and the relative intensities of γ rays. Typical gated spectra of ^{33}S are shown in Fig. 1.

We have added a few new levels and connecting γ transitions (Fig. 2) in the existing level scheme [16]. All these new transitions were totally shifted. To place these transitions in the level scheme, an angle-dependent 90° vs 90° symmetric γ-γ matrix was used. Apart from these, a few transitions previously reported in light-ion-induced experiments [1] were observed also for the first time in heavy ion fusion reaction.

The multipolarity of the γ-ray transition was determined from directional correlation of γ rays emitted from the excited oriented state (DCO) measurements. The DCO ratio ($R_{\rm DCO}$) [18] of a γ transition (γ_1) is defined as the ratio of intensities of that γ ray [$I(\gamma_1)$] for two different angles in coincidence with another γ ray (γ_2) of known multipolarity. It is given by

$$R_{\rm DCO} = \frac{I^{\gamma_1} \text{ observed at } \theta, \text{ gated by } \gamma_2 \text{ at } 90^\circ}{I^{\gamma_1} \text{ observed at } 90^\circ, \text{ gated by } \gamma_2 \text{ at } \theta}.$$

In our experiment, DCO ratios for most of the transitions have been determined for $\theta = 157^\circ$ (Table I). For the

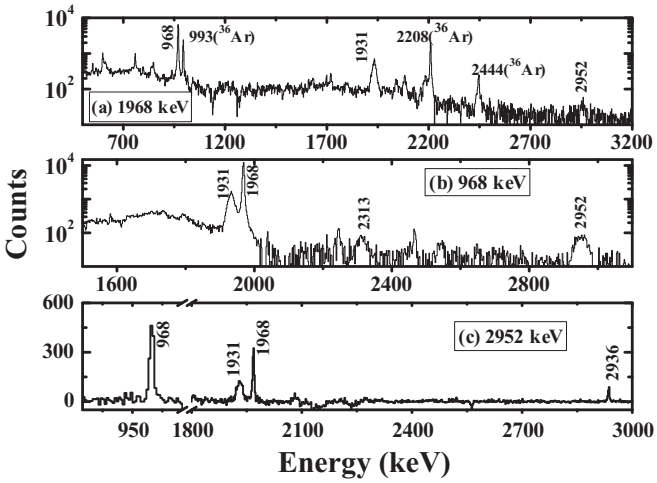

FIG. 1. Typical background subtracted coincidence spectra obtained by putting gates on (a) 1968-keV, (b) 968-keV, and (c) 2952-keV transitions. 1968-keV gated spectra contain contaminant peaks from ^{36}Ar marked in the figure. These γ rays are in coincidence with 1970-keV ($2^+ \rightarrow 0^+$) transition in ^{36}Ar.

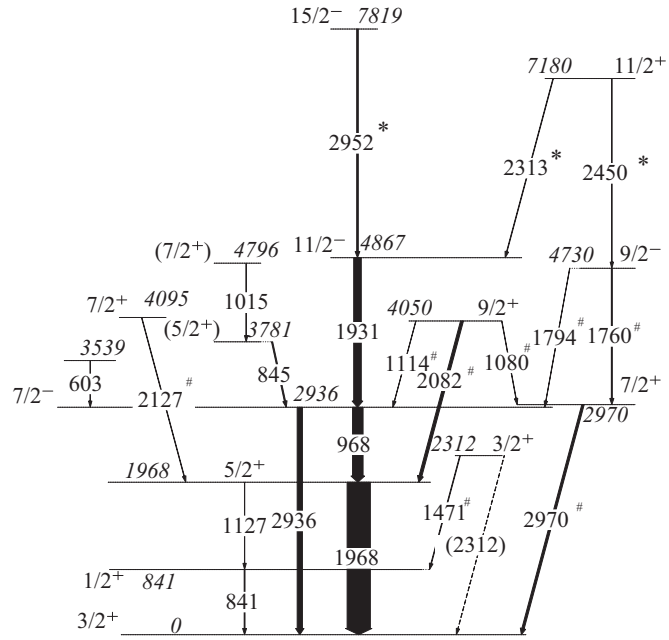

FIG. 2. Partial level scheme of ^{33}S. Newly assigned γ transitions and those observed in light-ion-induced reactions are indicated by ∗ and #, respectively.

assignment of spins and the γ-ray multipole mixing ratios (δ), the experimental DCO values have been compared with the theoretical values calculated by using the computer code ANGCOR [18]. The spin alignment parameter $\sigma/J = 0.3$, similar to our earlier work [2] was used for this calculation.

The integrated polarization asymmetry measurements (IPDCO) [19] have also been carried out to determine the electric or magnetic nature of the transitions. Two matrices containing information about parallel and perpendicular scattering, respectively [2], have been constructed for the IPDCO measurement. The other necessary details of the analysis of polarization data have been discussed in Ref. [2].

The relative intensities, experimental $R_{\rm DCO}$ values, mixing ratios (for mixed transitions), and experimental and theoretical polarization asymmetry values for transitions in ^{33}S are listed in Table I. The maximum uncertainty in most of the γ energy is $\leqslant$1 keV. However, for totally shifted γ peaks, the error may be more. Uncertainties quoted in intensities and branching ratios (Table II) are only statistical errors. The relative intensities of these transitions have been estimated primarily from 1968-keV gated spectrum. The branching ratios of the decay-out transitions of 1968 and 2936 keV levels have been determined from 968 and 1931 keV gated coincidence spectra, respectively (Table II). The results have been compared with previous data [1] and the theoretical branching ratios obtained from shell model calculations. Necessary corrections to include de-excitation via transitions parallel to 1968 keV have been included by using these branching ratios, wherever possible. Because 1127 keV is a very weak transition (branching <1%), no branching correction was included for the intensities of 2082- and 2127-keV transitions. However, the relative intensities of 845-, 1015-, 1114-, 1931-, 2313-, and 2952-keV

TABLE I. Relative intensity (I_{rel}), R_{DCO}, Δ_{IPDCO}, and the mixing ratio (δ) of the γ transitions in ^{33}S.

E_γ	I_{rel}	J_i	J_f	Gating γ		R_{DCO}	Mixing ratio (δ)			Δ_{IPDCO}	
(keV)				E(keV)	ΔJ		Present	Previous[1]	Theor.	Expt.	Calc.
841	>3.2	$1/2^+$	$3/2^+$	1127	2	1.2(3)	–	0.18	0.19	−0.13(3)	–
845	5.0(2)	$(5/2^+)$	$7/2^-$	968	1	1.0(2)	0.1(5)		0	0.02(1)	0.02
968	45.2(3)	$7/2^-$	$5/2^+$	1931	2	0.52(1)	0.02(4)	− 0.04(4)	0.02	0.05(2)	0.05
1015	0.8(3)	$(7/2^+)$	$(5/2^+)$	968	1	1.1(4)	0.1(2)		0.14	−0.04(3)	−0.05
1080	1.4(1)[a]	$9/2^+$	$7/2^+$	2970	2	0.35(3)	−0.09(2)	−0.33(4)	0.96	−0.02(1)	−0.03
1114	1.7(2)	$9/2^+$	$7/2^-$					$E1$	0	0.04(1)	0.04
1127	0.7(2)[b]	$5/2^+$	$1/2^+$	968	1	1.5(3)		$E2$	0		
1471	2.5(2)	$3/2^+$	$1/2^+$	841	1	1.06(9)		−0.12(10)	0.34	−0.04(1)	−0.04[c]
1760	4.2(1)	$9/2^-$	$7/2^+$	2970	2	0.47(2)	0.05(2)	−0.02(3)	−0.02	0.05(1)	0.03
1931	32.6(6)	$11/2^-$	$7/2^-$	968	1	1.9(1)	$E2$		0	0.05(1)	0.03
1968	100(2)	$5/2^+$	$3/2^+$	968	1	0.59(1)	−1.41(4)	−0.60(12)	−1.5	−0.004(1)	0.02
2082	12.2(3)	$9/2^+$	$5/2^+$	1968	1	2.1(2)[d]	$E2$	−0.02(3)	0	0.04(1)	0.03
2127	1.8(1)	$7/2^+$	$5/2^+$	1968	1	3.7(9)	0.3(1)	0.19(2)	0.30		
2313	2.1(3)	$11/2^+$	$11/2^-$	968	1	2.05(8)	−0.03(3)		0	0.01(1)	0.03
2450	0.4(2)	$11/2^+$	$9/2^-$	1760	1	1.1(2)	0.07(5)				
2936	22.6(7)[b]	$7/2^-$	$3/2^+$	2952	2	1.10(8)	−0.11(9)	−0.32(17)	0.04	− 0.04(1)	
2952	6.8(5)	$15/2^-$	$11/2^-$	968	1	1.9(1)	$E2$		0	0.014(2)	0.015
2970	7.5(3)	$7/2^+$	$3/2^+$	1760	1	1.72(8)	$E2$	$E2$	0	0.04(1)	0.02

[a]Estimated from branching ratios [1].
[b]Estimated from branching ratios (Table II).
[c]Using mixing ratio (δ) from Ref. [1].
[d]Estimated from 90°–65° matrix.

transitions, obtained from the 1968-keV gated spectrum, have been corrected with the branching of the 2936-keV transition. For 1968 keV and the transitions parallel to 1968 keV, relative intensities have been measured from the total projection spectrum and normalized with the 968-keV transition. The calculated mixing ratios for few transitions have also been compared with earlier measurements [1], wherever available (Table I). Because the 1794-keV transition was very weak, the spectroscopic information of this transition is not listed in Table I. In the present experiment, for the first time, we have measured the polarization asymmetry (Δ_{IPDCO}) for more than 10 γ transitions in ^{33}S.

1. *Levels with excitation energy ⩽3 MeV*

At low excitation energy (⩽3 MeV), two levels (2312 and 2970 keV) have been included in the excitation spectra of ^{33}S [16] populated in heavy-ion reactions. These levels were already observed in light-ion-induced experiments [1]. The spins and parities of these levels have been confirmed from DCO and polarization measurements. The 1471-keV transition emitted while deexciting the 2312-keV level was observed in the present experiment. However, the 2312-keV transition could not be confirmed because of lack of appropriate gating transition to distinguish it from the 2313-keV transition present at higher excitation energies. Therefore, in Fig. 2, this transition was marked by a dotted line.

TABLE II. Comparison of experimental and theoretical branching ratios of different excited levels.

Energy (keV)		Branching ratio		
Level	E_γ	Expt.		Theor.
		Present	Previous [1]	
1968	1127	0.7(2)	7(1)	1.5
	1968	99.3(3)	93(1)	98.5
2936	968	67(1)	51.8(15)	28
	2936	33(1)	48.2(21)	72

2. *Levels with excitation energy ⩾3 MeV*

Three excited levels at 4050, 4095, and 4730 keV, already observed in light ion experiments, were also observed in our experiment. The spin-parity assignments of these levels have been confirmed from present measurements.

From an earlier experiment [16], spin parity of two other levels at 3781 keV and 4796 keV have been tentatively assigned as $(9/2^+)$ and $(11/2^-)$, respectively. These assignments were based on the electric dipole nature of both 845- and 1015-keV decay out transitions. In the present experiment, we have confirmed that both transitions are dipole in nature. However, positive Δ_{IPDCO} for the 845-keV transition and negative Δ_{IPDCO} for the 1015-keV transition (Table I) indicated that these transitions have electric and magnetic characters, respectively. So, the previous parity assignment of the 4796-keV level was changed. If we consider the previous spin assignments [i.e., the 3781-keV level as $(9/2_1^+)$ and the 4796-keV level as $(11/2_1^+)$], the experimental and calculated (shell model) excitation energies show large differences (Option I in Table III). On the other hand, calculated and experimental excitation energies of these levels as well as neighboring ones

TABLE III. Comparison of experimental and theoretical results for different spin assignments of the 3781- and 4796-keV excited levels. The level at 2868 keV [1] marked with * is not observed in the present experiment.

J^π	E_x (keV)		J^π	E_x (keV)	
	Expt.	Theor.		Expt.	Theor.
Option I					
$(9/2_1^+)$	3781	4243	$(11/2_1^+)$	4796	6732
$9/2_2^+$	4050	5965	$11/2_2^+$	7180	7372
Option II					
$5/2_1^+$	1968	1895	$7/2_1^+$	2970	2891
$5/2_2^+$	2868*	2839	$7/2_2^+$	4095	3973
$(5/2_3^+)$	3781	3899	$(7/2_3^+)$	4796	5083
$9/2_1^+$	4050	4243	$11/2_1^+$	7180	6732

match reasonably well if we assign the 3781-keV level as $5/2^+$ (Option II in Table III). The spin-parity assignments of these levels have been changed tentatively (Fig. 2). In the previous level scheme, the spin and parity of the 3539-keV level deexciting by a weak 603-keV transition was not assigned [16]. However, in the present experiment, this level could not be confirmed as the 603-keV transition could not be separated from the broad 598-keV peak arising from the interaction of neutrons with the Ge detectors. The spin and parity of another excited level at 4867 keV [16] were not assigned. In the present work, $J^\pi = 11/2^-$ was assigned to this level from the $R_{\rm DCO}$ and polarization asymmetry measurement of the decay out γ transition (1931 keV) (Table I). Apart from these, two new levels at 7180- and 7819-keV excitation energy with spin parity $11/2^+$ and $15/2^-$, respectively, and three new transitions have been added to the existing level scheme [16] in this energy domain.

3. *Modification in the level scheme*

In previous work [16], two 597-keV transitions were sequentially placed in the level scheme, de-exciting from the 5990- and 5393-keV levels. The spin parities of these levels were not assigned. In the present work, these levels have been excluded. It was found that these 597-keV γ transitions are originated from the ^{74}Ge$(n,n')^{74}$Ge reaction [1]. To justify this claim, a 597-keV gated spectrum was generated and normalized with the total projection spectrum (Fig. 3). We have observed that γ transitions emitted by nuclei which were populated through neutron emission channels, like ^{34}Cl (αn), ^{36}Cl (2pn), ^{37}Ar (np), etc., have similar intensities in both the 597-keV gated and the total projection spectra. However, for those belonging to ^{37}Ar which are in coincidence with a 598-keV transition in its level scheme, viz., the intensities of 680- and 937-keV transitions, etc., are much higher in the 597-keV gated spectrum than the total projection spectrum. On the other hand, for γ rays emitted by nuclei which were populated through emission of charged particles only, almost zero intensities have been observed in the 597-keV gated spectrum, viz., the 2127- and 2561-keV transitions in ^{34}S (α p) (Fig. 3). In this present experiment, ^{33}S was populated through the ^{27}Al(^{12}C,αpn)^{33}S reaction, i.e., a neutron emission channel. So, if 597-keV transitions were present in the ^{33}S level scheme

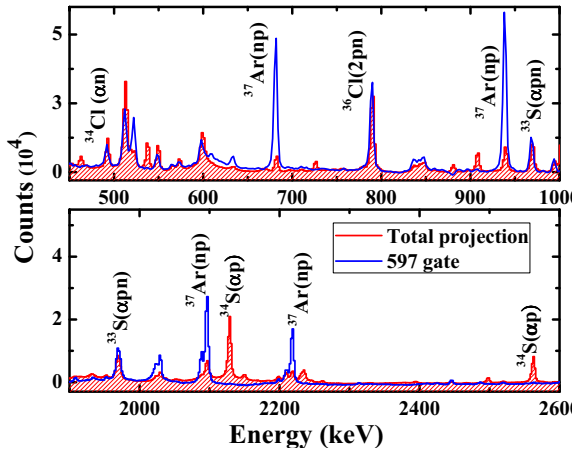

FIG. 3. (Color online) Total projection (shaded plot with red border) and normalized 597-keV gated (blue line) spectra obtained from our experiment. γ peaks have been marked with names of deexciting nuclei along with the names of emitted particles in that particular reaction channel within the parentheses.

like ^{37}Ar, we can expect more intense 968-keV and 1968-keV peaks in the 597-keV gated spectrum than the total projection spectrum. However, these transitions have almost equal intensities like γ rays emitted from ^{34}Cl, ^{36}Cl, etc., in both spectra as shown in Fig. 3. In the previous experiment [16] also, ^{33}S was populated through a neutron emission channel reaction. Therefore, from these observations, a modification in the previous level scheme was made by excluding these two levels.

B. Lifetime measurement

Several Doppler shifted γ peaks have been observed in the spectra for ^{33}S. These indicate the presence of states with short half lives. Few of these transitions were totally shifted. The lifetimes of these states have been measured using the Doppler shift attenuation method (DSAM). Two asymmetric matrices having events from a particular angle (157° or 65°) on one axis and the coincidence events from the 90° detectors on the other have been constructed to generate the lineshape spectra. A modified version of computer code LINESHAPE [20,21] which included corrections for the broad initial recoil momentum distribution produced by the α-particle evaporation, was used to extract the level lifetimes from these Doppler shifted spectra. The initial recoil momenta distributions of ^{33}S have been obtained from statistical model code PACE4 [22]. Shell corrected Northcliffe & Schilling stopping powers [23] have been used for calculating the energy loss of ions in matter. We have discussed other necessary details of lineshape analysis in our earlier work on ^{34,35}Cl [2,3].

In the present experiment, we have extracted the lifetimes of the 4867-, 7819-, and 7180-keV levels by analyzing the lineshapes of the de-exciting γ's (1931 keV, 2952 keV, and 2313 keV, respectively). The lineshape spectra (Fig. 4) of the decay out transitions from these levels have been generated for three different angles (157°,90°, and 65°). Unlike the usual procedure of generating the angle-dependent lineshape spectra by putting gates on γ's above the transition (GTA) of

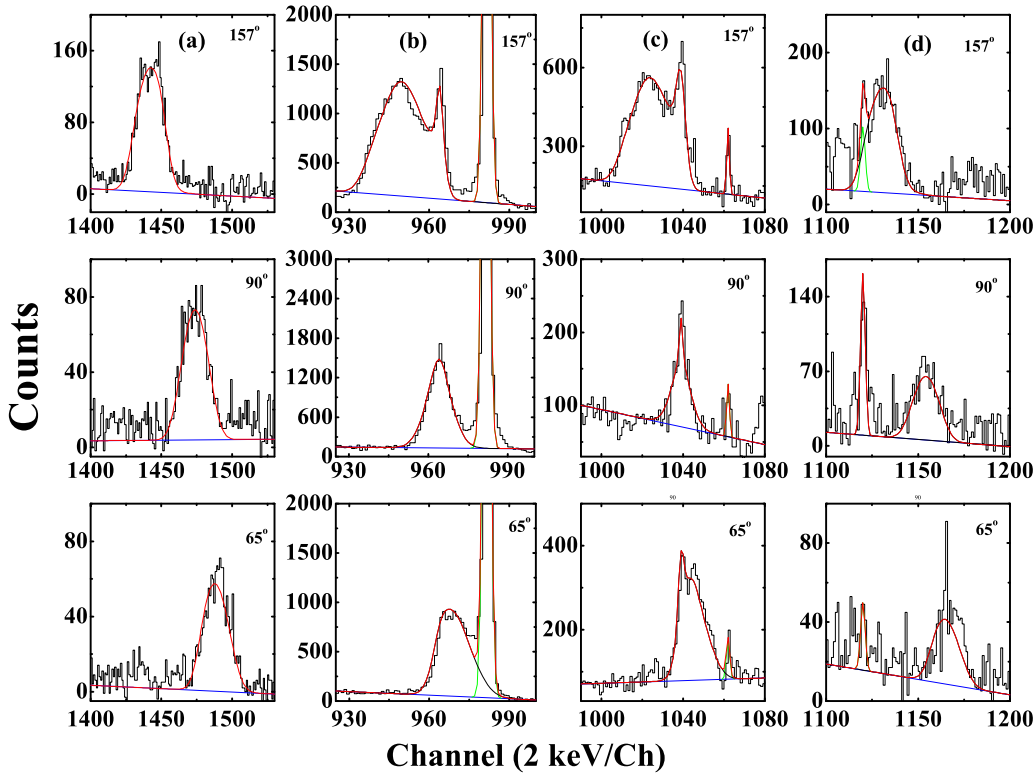

FIG. 4. (Color online) Experimental (black) and simulated (red) lineshape spectra are shown for (a) 2952-keV, (b) 1931-keV, (c) 2082-keV, and (d) 2313-keV transitions for different angles as mentioned in the figure.

interest, these spectra have been generated by putting gates on transitions below the Doppler shifted transition (GTB) as these spectra have better statistics. Therefore, we had to consider the side feeding effects with proper care, similar to our earlier work [2]. The lineshape spectra of the 2952- and 1931-keV transitions [Figs. 4(a) and 4(b)] were fitted simultaneously as members of a single band. The rotational cascade side feeding with five transitions was considered, assuming 100% feeding to the topmost level of the band. So, we could only set the upper limit of the mean life of the 7819-keV level. Similarly, for the 7180-keV level [the 2313-keV transition in Fig. 4(d)], the upper limit of its mean life was obtained, as no feeding transitions to this level were observed in the present work (Fig. 2).

We have also estimated the lifetimes of the 4730- and 4050-keV levels. The lifetimes of these levels were previously measured by Carr *et al.* through the ^{30}Si(α,n)^{33}S reaction [9]. They had included 25% error in the measured lifetimes because of the uncertainty in the estimation of slowing down time. In the present work, for the 4050-keV level [the 2082-keV transition in Fig. 4(c)], the upper limit of the measured lifetime was comparable to the earlier results. However, for the 4730-keV level (the 1760-keV transition in Fig. 5), the lifetime extracted from our measurement was more than twice the previous value. The corresponding experimental $B(E1)$ strength of the 1760-keV transition for this new lifetime is comparatively closer to the calculated $B(E1)$ value (Table VI) than the earlier measurement. If we considered the lifetime from previous data [1], the corresponding experimental $B(E1)$ strength of 1760 keV comes out to be almost 7 times larger than the calculated value (Table VI). However, even from the present measurement, the experimental $B(E1)$ is substantially larger than the theoretical value.

IV. EVOLUTION OF COLLECTIVITY

In ^{33}S, a sequence of three levels (7819, 4867, and 2936 keV) connected by $E2$ transitions, was observed. The reduced transition probabilities of these transitions have been

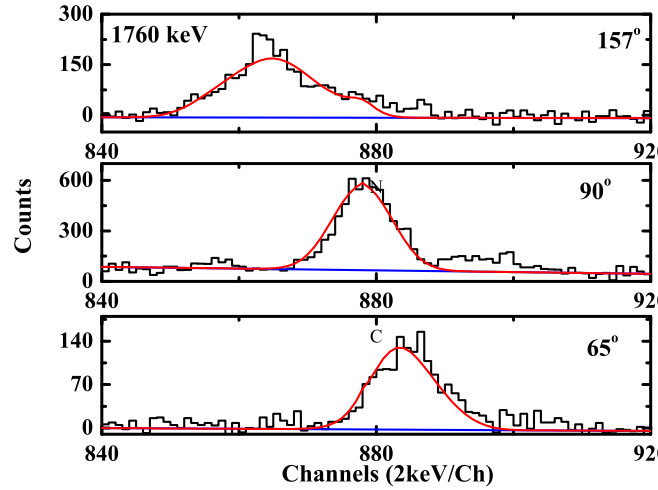

FIG. 5. (Color online) Experimental (black) and simulated (red) lineshape spectra are shown for the 1760-keV transition for different angles as indicated in the figure.

calculated from their measured lifetimes. The $B(E2)$ values of the 1931- and 2952-keV transitions were 16(3) and >28 W.u., respectively, indicating the presence of collectivity at these excitation energies. The deformation parameters β_2 [24] corresponding to the $B(E2)$'s for the 1931- and 2952-keV transitions are 0.29 and 0.37, respectively, indicating an increase in collectivity with spin along this sequence. This band may therefore evolve to a superdeformed rotational band similar to the negative parity yrast band in ^{35}Cl [3] at relatively higher spins. On the other hand, the strong $B(E1)$ value discussed in the earlier section may also indicate the possibility of the presence of a cluster structure in ^{33}S similar to that in ^{35}Cl [3]. Therefore, for a firm conclusion, extension of the level scheme to higher spins along with improved measurements of level lifetimes for similar states is essential.

V. THEORETICAL CALCULATION

To know the microscopic origin of each excited state in ^{33}S, large basis shell model calculations have been performed using the code OXBASH [25]. The valence space consists of $1d_{5/2}$, $1d_{3/2}$, $2s_{1/2}$, $1f_{7/2}$, $1f_{5/2}$, $2p_{3/2}$, and $2p_{1/2}$ orbitals for both neutron and protons above the ^{16}O inert core. The number of valence particles (protons + neutrons) in ^{33}S is 17. The *sdpfmw* interaction [26] (as referred to within the OXBASH code package) was used for the calculation. Other relevant details of the interaction and calculation are discussed in [27].

It is almost impossible to perform unrestricted calculations in the full valence space for nuclei having such a large number of valence particles. Therefore several truncation schemes have to be adopted for reproduction of the experimental data. In the next sections, different truncation schemes and their regions of applicability for our experimental data will be discussed.

A. Positive parity states

Large basis shell model calculation with $0\hbar\omega$ excitation was performed to generate the positive parity states in ^{33}S. In this truncation scheme, full *sd* shell was used as model space. The maximum angular momentum state in ^{33}S, which can be generated in this model space is $23/2^+$. In the present level scheme, maximum observed angular momentum state (positive parity) was $11/2^+$. All the positive parity states were reproduced quite accurately with $0\hbar\omega$ excitation (Fig. 6). The calculated ground-state binding energy of ^{33}S was −191.139 MeV which agrees well with the experimental binding energy −191.264 MeV (corrected for Coulomb energy) [28]. In the calculation, the mass normalization factor (usually given by the number of valence particles in the *sd* shell) for the *sd* shell two-body matrix elements (tbme) was 33.

B. Negative parity states

For the negative parity states, 1p-1h excitation (Theo-Neg1) was considered. In this truncation, only one nucleon was allowed to be excited into the next *pf* shell with rest of the valence nucleons distributed in the orbitals of the *sd* shell without any restriction; 32 was taken as the mass normalization factor for *sd* shell tbme's for this calculation. However, except for the $9/2^-$ state, the calculated energies are lower than the

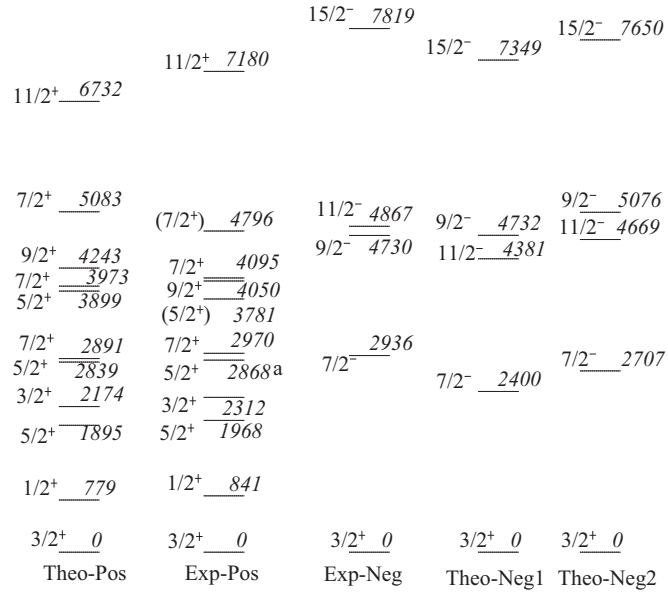

FIG. 6. Comparison of theoretical and experimental level schemes for positive and negative parity states in ^{33}S. All these energies are plotted considering the ground-state energy (−191.139 MeV) as 0. Level marked as **a** was not observed in the present experiment.

experimental values by ∼0.5 MeV (Fig. 7). It indicates that with this mass normalization and unrestricted occupation of the *sd* orbitals with at least four nucleons in $1d_{5/2}$ orbital, configuration mixing is too large to underpredict the energy. On the other hand if the mass normalization factor is taken to be 33 (Fig. 7), the calculated energies are overpredicted. In Ref. [27], this overprediction was corrected by reduction of single particle energies of the *pf* orbitals [27]. Instead of

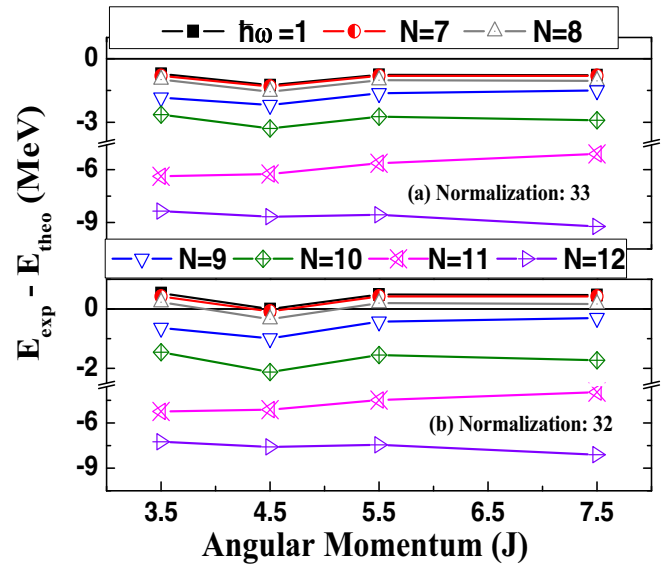

FIG. 7. (Color online) Differences between the experimental and calculated energies of negative parity states for (1p-1h) excitation with different restrictions in the occupation of the $1d_{5/2}$ orbital. The mass normalization factor for the *sd* shell is (a) 33 and (b) 32.

TABLE IV. Structure of the wave functions for full *sd* shell calculation. The partitions are given in terms of occupation numbers of single particle valence states in the following order: $1d_{5/2}$, $1d_{3/2}$, and $2s_{1/2}$. Those with >10% contribution in the wave function are shown in the table. N_1 is the total number of particle partitions, each of which contribute >1%. N_2 gives the minimum number of particle partitions, each of which contribute $\leqslant$1%.

J_i^π	T	Energy (MeV)		Wave function		N_1	N_2
		Expt.	Theor.	%	Partition		
$3/2_1^+$	1/2	0 (−191.264)	0 (−191.139)	42	[12,1,4]	13	3
				18	[10,3,4]		
				15	[12,3,2]		
$1/2_1^+$	1/2	0.841	0.779	40	[12,2,3]	14	2
				16	[10,4,3]		
				12	[12,4,1]		
$5/2_1^+$	1/2	1.968	1.895	34	[12,2,3]	12	5
				16	[12,4,1]		
				14	[11,3,3]		
				12	[10,4,3]		
$3/2_2^+$	1/2	2.312	2.174	25	[12,3,2]	13	5
				16	[12,2,3]		
$5/2_2^+$	1/2	2.867	2.839	19	[12,3,2]	13	5
				18	[11,2,4]		
				10	[11,4,2]		
$7/2_1^+$	1/2	2.970	2.891	38	[12,2,3]	12	4
				12	[11,3,3]		
				11	[10,4,3]		
$(5/2_3^+)$	1/2	3.781	3.899	16	[11,3,3]	15	3
				12	[11,4,2]		
				11	[12,2,3]		
				11	[11,2,4]		
$9/2_1^+$	1/2	4.050	4.243	35	[11,2,4]	12	2
				22	[12,3,2]		
				12	[11,4,2]		
$7/2_2^+$	1/2	4.095	3.973	20	[11,2,4]	15	3
				15	[12,3,2]		
				10	[11,4,2]		
				10	[11,3,3]		
$(7/2_3^+)$	1/2	4.796	5.083	26	[11,3,3]	12	4
				17	[12,4,1]		
				14	[12,3,2]		
$11/2_1^+$	1/2	7.180	6.732	24	[11,2,4]	10	2
				17	[10,3,4]		
				16	[11,3,3]		
				11	[11,4,2]		
				10	[9,4,4]		

modifying the single particle energies, in this work we have restricted the number of valence nucleons in $1d_{5/2}$ orbital for both the mass normalizations to understand the effect. In Fig. 7, we have plotted the differences between the experimental and calculated energies. The calculated excitation energies for the negative parity states in ^{33}S show best agreement with experimental data for $[(1d_{5/2})^{8-12}(1d_{3/2}2s_{1/2})^{4-8}\ (pf)^1]$ particle restriction (Fig. 6, Theo-Neg2) with the normalization factor equaling 32.

C. Configuration mixing and collectivity

The decomposition of the wave functions in terms of particle partitions as discussed in detail in our earlier work [2] have been tabulated in the Tables IV and V. Most of the positive parity states show substantial configuration mixing. It is found (Table IV) that positive parity states have the contributions from 10 to 15 particle partitions, each having at least 1% contribution. The largest contribution from a single partition ranges from 16% to 42%. These wave functions can be compared with those [27] for the positive parity states in ^{35}Cl. The yrast positive parity states in ^{35}Cl have a much smaller extent of configuration mixing. The largest contribution from a single partition was in the range of 40%–70%. On the other hand, a similar extent of configuration mixing was already observed in mid-*sd* shell nuclei, like ^{34}Cl [2] and ^{30}P [29].

Negative parity states, especially the members of the negative signature band in ^{33}S have more configuration mixing

TABLE V. Structure of the wave functions for (1p-1h) excitation in *sd-pf* shell calculation (Theo-Neg1). The partitions are given in terms of occupation numbers of single particle valence states in the following order: $1d_{5/2}$, $1d_{3/2}$, $2s_{1/2}$, $1f_{7/2}$, $1f_{5/2}$, $2p_{3/2}$, and $2p_{1/2}$. See the caption of Table IV for detail.

J_i^π	T	Energy (MeV)		Wave function		N_1	N_2
		Expt.	Theor.	%	Partition		
$7/2_1^-$	1/2	2.936	2.400	17	[12,2,2,1,0,0,0]	19	11
				16	[12,0,4,1,0,0,0]		
				12	[10,2,4,1,0,0,0]		
$9/2_1^-$	1/2	4.730	4.732	16	[12,1,3,1,0,0,0]	17	11
				13	[12,3,1,1,0,0,0]		
				11	[11,2,3,1,0,0,0]		
				11	[10,3,3,1,0,0,0]		
$11/2_1^-$	1/2	4.867	4.381	17	[12,1,3,1,0,0,0]	16	12
				14	[12,3,1,1,0,0,0]		
				11	[10,3,3,1,0,0,0]		
$15/2_1^-$	1/2	7.819	7.349	18	[12,2,2,1,0,0,0]	16	8
				12	[11,3,2,1,0,0,0]		
				12	[11,1,4,1,0,0,0]		

(Table V) in their wave function structure; 16–19 particle partitions with the largest contribution ranging from 16% to 18% have been observed for these states.

The reduced transition probabilities [$B(E1)$, $B(M1)$, and $B(E2)$] for a few transitions have been calculated by using the effective charges $e_p = 1.5$ e and $e_n = 0.5$ e and free values of g factors. Most of the calculated values show good agreement with the corresponding experimental data (Table VI), which provide an evidence in favor of the reliability of the calculated wave functions. For the negative parity negative signature band, the calculated $B(E2)$ value (11.3 W.u.) for the 1931-keV transition has good agreement with experimental $B(E2)$. However, for the 2952-keV transition, the large difference between theoretical and experimental $B(E2)$s indicates the need for inclusion of other configurations. Hence calculations with 3p-3h configuration have been carried out for these negative parity states. As 3p-3h calculation with the full *sd-pf* model space is not possible because of the large matrix dimension, two different particle truncations in $1d_{5/2}$ orbital have been adopted for these calculations. The calculated transition energies and the $B(E2)$ values are plotted in Figs. 8 and 9. In ^{33}S, the number of valence particles is 17 and for 3p-3h excitation, we have only 14 nucleons in the *sd* shell. Therefore, in calculations with the filled-up $1d_{5/2}$ orbital with 12 (11) nucleons, only 2 (3) active nucleons are present in the *sd* space, inadequate for generating large collectivity. The calculations also indicate (Fig. 9) that the $B(E2)$s increase with an increase in the number of active particles in *sd* orbitals. The calculated $B(E2)$ strength for the 2952-keV transition may be improved by increasing the number of active particles in *sd* orbitals, which is presently beyond our computational abilities. Moreover, further experimental data later may show that the higher spin states of this negative parity band arising from 3p-3h excitations to the *pf* shell evolve to a superdeformed structure for ^{33}S, similar to that observed for ^{35}Cl [3]. This will indicate that for this 2952-keV transition, a mixing of 1p-1h and 3p-3h configurations may be needed. It was also noted earlier that in ^{35}Cl, ^{36}Ar, and ^{40}Ca, the calculations [3] failed dramatically to reproduce the transition probabilities for the states where different configurations interact to their maximum.

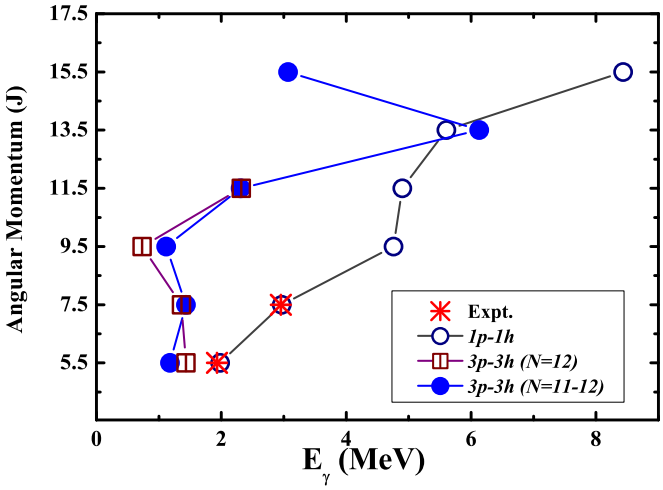

FIG. 8. (Color online) Experimental and calculated transition energies of the negative parity band in ^{33}S. The theoretical values corresponding to (1p-1h) and (3p-3h) excitation with $N = 12$ and $N = 11$–12 nucleons in the $1d_{5/2}$ orbitals are shown.

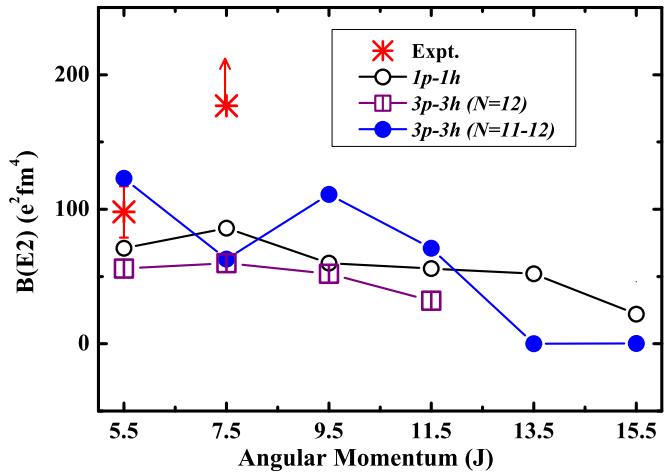

FIG. 9. (Color online) Experimental and calculated $B(E2)$ values in e^2fm^4 of the negative parity band in ^{33}S. The theoretical values corresponding to (1p-1h) and (3p-3h) excitation with $N = 12$ and $N = 11$–12 nucleons in the $1d_{5/2}$ orbitals are shown.

VI. CONCLUSION

The level scheme of ^{33}S, populated through the ^{27}Al(^{12}C,αpn)^{34}Cl reaction, was extended up to 8 MeV by including a few levels in the existing level scheme. Apart from these a few excited levels which were already reported in light-ion-induced experiments, were also observed. The spin parities of all levels in the new level scheme have been assigned

TABLE VI. Comparison of experimental and theoretical (Theo-Pos and Theo-Neg1) reduced transition probabilities for different transitions in ^{33}S.

E_X	$\tau_{\rm mean}$(ps)		J_i^π	E_γ	J_f^π	$B(E1)(\times 10^{-6}e^2\text{fm}^2)$		$B(M1)\left(\times 10^{-3}\mu_N^2\right)$		$B(E2)(e^2\text{fm}^4)$	
keV	Reported [1]	Present work		keV		Expt.	Theor.	Expt.	Theor.	Expt.	Theor.
841	1.66(17)	–	$1/2_1^+$	841	$3/2_1^+$			55(8)	31	36(5)	23
1968	0.136(20)	–	$5/2_1^+$	1127	$1/2_1^+$					23(6)	22
			$5/2_1^+$	1968	$3/2_1^+$			18(3)	8	128(23)	65
2936	40.7(20)	–	$7/2_1^-$	968	$5/2_1^+$	11(1)	10	0.56(4)*	0.52*		
2970	0.085(12)	–	$7/2_1^+$	2970	$3/2_1^+$					41(7)	39
4050	0.305(77)	<0.38	$9/2_1^+$	2082	$5/2_1^+$					>47	60
4730	0.082(22)	0.19(4)	$9/2_1^-$	1760	$7/2_1^+$	493(120)	182	46(12)*	2*		
4867	–	0.30(5)	$11/2_1^-$	1931	$7/2_1^-$					98(19)	71
7180	–	<0.08	$11/2_1^+$	2313	$11/2_1^-$	>315	29				
7819	–	<0.02	$15/2_1^-$	2952	$11/2_1^-$					>177	86

* $B(M2)$ in $\mu_N^2\text{fm}^2$.

or confirmed from DCO and polarization measurements. Lifetimes of a few levels have also been determined from lineshape analysis using the DSAM technique. Large basis shell model (LBSM) calculations have been performed for different truncations to understand the microscopic origin of these levels. A band consisting of three levels connected by strong $E2$ transitions and large $B(E2)$ values with 1p-1h excitation to the pf shell, may evolve into a superformed band at higher spins with 3p-3h excitation. Large configuration mixing and $B(E2)$ values obtained from shell model calculations also supported this assignment. However, $B(E2)$ for the topmost transition could not be reproduced in theory because of limitations in computational capabilities.

ACKNOWLEDGMENTS

The authors sincerely thank P. K. Das (SINP), S. K. Jadhav (TIFR), and P. B. Chavan (TIFR) for their technical help before and during the experiment. Thanks are due to the target laboratory of VECC, Kolkata for preparation of the target. Special thanks are due to the Pelletron staff for nearly uninterrupted beam. One of the authors (A.B.) was financially supported by Council of Scientific and Industrial Research (CSIR), India, under Contract No. 09/489(0068)/2009-EMR-1. Finally, we would like to thank all the members of the INGA (partially funded by the Department of Science and Technology, Government of India, Grant No. IR/S2/PF-03/2003-I) collaboration.

[1] http://www.nndc.bnl.gov.
[2] Abhijit Bisoi *et al.*, Phys. Rev. C **89**, 024303 (2014), and references therein.
[3] Abhijit Bisoi *et al.*, Phys. Rev. C **88**, 034303 (2013), and references therein.
[4] C. E. Svensson *et al.*, Phys. Rev. Lett. **85**, 2693 (2000); Phys. Rev. C **63**, 061301(R) (2001).
[5] E. Ideguchi *et al.*, Phys. Rev. Lett. **87**, 222501 (2001); C. J. Chiara *et al.*, Phys. Rev. C **67**, 041303 (R) (2003).
[6] E. Caurier, F. Nowacki, and A. Poves, Phys. Rev. Lett. **95**, 042502 (2005); E. Caurier, J. Menèndez, F. Nowacki, and A. Poves, Phys. Rev. C **75**, 054317 (2007).
[7] P. M. Endt and R. B. Firestone, Nucl. Phys. A **633**, 1 (1998).
[8] R. S. Cox *et al.*, Phys. Rev. **175**, 1419 (1968).
[9] P. E. Carr *et al.*, J. Phys. A: Math., Nucl. Gen. **6**, 685 (1973).
[10] H. Molique, J. Dobaczewski, and J. Dudek, Phys. Rev. C **61**, 044304 (2000).
[11] M. Kimura and H. Horiuchi, Phys. Rev. C **69**, 051304(R) (2004).
[12] Takatoshi Ichikawa, Yoshiko Kanada-Enýo, and Peter Möller, Phys. Rev. C **83**, 054319 (2011).
[13] K. Ikeda, N. Takigawa, and H. Horiuchi, Prog. Theo. Phys. Suppl. extra number **464**, (1968).
[14] K. Morita *et al.*, Phys. Rev. Lett. **55**, 185 (1985); Shigeo Ohkubo and Kotoe Yamashita, Phys. Rev. C **66**, 021301(R) (2002); S. Ohkubo, Nucl. Phys. A **722**, 414 (2003); M. Itoh *et al.*, Phys. Rev. C **88**, 064313 (2013).
[15] D. G. Jenkins *et al.*, Phys. Rev. C **86**, 064308 (2012); J. Darai, J. Cseh, and D. G. Jenkins, *ibid.* **86**, 064309 (2012).
[16] R. Chakrabarti *et al.*, Phys. Rev. C **80**, 034326 (2009).
[17] R. Palit, Proceedings DAE-BRNS Symp. on Nucl. Phys. (India) **55**, I11 (2010), http://www.sympnp.org/proceedings/; R. Palit *et al.*, Nucl. Instrum. Methods A **680**, 90 (2012).
[18] E. S. Macias, W. D. Ruhter, D. C. Camp, and R. G. Lanier, Comput. Phys. Commun. **11**, 75 (1976).
[19] K. Starosta *et al.*, Nucl. Instrum. Methods A **423**, 16 (1999).
[20] J. C. Wells and N. R. Johnson, in Report ORNL-6689 (Oak Ridge National Laboratory, Oak Ridge, 1991), p.44.
[21] R. K. Bhowmik (private communication).
[22] A. Gavron, Phys. Rev. C **21**, 230 (1980).
[23] L. C. Northcliffe and R. F. Schilling, Nucl. Data Tables **7**, 233 (1970).
[24] http://www.physics.mcmaster.ca/~balraj/sdbook.
[25] B. A. Brown, A. Etchegoyen, W. D. M. Rae, and N. S. Godwin, MSU-NSCL Report No. 524 (National Superconducting Cyclotron Laboratory, Michigan State University, East Lansing, 1985).
[26] E. K. Warburton, J. A. Becker, and B. A. Brown, Phys. Rev. C **41**, 1147 (1990).
[27] R. Kshetri *et al.*, Nucl. Phys. A **781**, 277 (2007).
[28] G. Audi, A. H. Wapstra, and C. Thibault, Nucl. Phys. A **729**, 337 (2003); B. J. Cole, J. Phys. G: Nucl. Phys. **11**, 351 (1985).
[29] Indrani Ray *et al.*, Phys. Rev. C **76**, 034315 (2007).